

Hybrid Multipole-Beam Approach to Electromagnetic Scattering Problems

Amir Boag, Eric Michielssen and Raj Mittra
Electromagnetic Communication Laboratory
Department of Electrical and Computer Engineering
University of Illinois, Urbana, IL 61801

ABSTRACT. *A hybrid technique combining the Complex Multipole Beam Approach (CMBA) with the Method of Moments (MoM) for the solution of the problems of electromagnetic scattering is presented in this paper. In this technique the CMBA provides for a substantial reduction in the matrix size by taking advantage of the essentially band-limited spatial spectrum of the scattered field in the vicinity of smooth surfaces, while the MoM is employed for the modeling of non-smooth or inhomogeneous regions within the problem geometry. The key step in the CMBA is to represent the scattered field in terms of a series of beams produced by multipole sources located in a complex space. The CMBA not only reduces the number of unknowns, but also generates a generalized impedance matrix with a banded structure and a low condition number. In the present hybrid technique, the scattering properties of each complex region, requiring a relatively large number of unknowns per unit volume, are described in terms of a Beam-matrix, which is constructed numerically to relate the amplitudes of outgoing beams to those of incoming ones. The proposed direct solution scheme takes into account the interactions between all of the complex regions and the smooth portions of the scatterer geometry using an algorithm similar to the recursive T-matrix approach. This hybrid technique, that combines the CMBA with other conventional methods, is a versatile tool, and is expected to enhance the scope of application of the CMBA to a much wider class of problems.*

1. INTRODUCTION

The conventional approach to formulating the problem of electromagnetic scattering using the Method of Moments (MoM) is to employ subdomain basis functions to represent the surface currents [1] on the body. This approach often requires the use of ten or more unknowns per linear wavelength, and thus leads to relatively large matrices even for moderately-sized scatterers. In addition, the resulting generalized impedance matrix is typically dense, owing to a strong coupling, or "reaction", between the subdomain basis and testing functions, even when they are remotely separated from one another. However, it is well-known from the asymptotic solutions of canonical problems, that wave interactions between the smooth parts of the scatterer are essentially local. Canning [2] has shown that, for smooth scatterers, the use of Gabor type of basis functions [3], viz., functions comprising of windowed exponentials, can introduce the desired impedance matrix localization (IML) feature in the matrix equation. It should be noted, however, that the localization of the matrix elements near the diagonal is achieved in this approach at the expense of a higher computational cost, introduced by the need to compute the

double integrals for the matrix elements that involve the special basis and testing functions. It is also worthwhile noting that the Gabor type of basis functions have been employed in the past for the analysis of coupling through narrow slots [4]; however, the computational savings achieved in this process were relatively meager due to the highly discontinuous nature of the slot coupling problem.

Two alternate approaches, also proposed recently, are the Multiple Multipole (MMP) [5] and the Current Model [6] methods, both of which exhibit a potential for substantial savings in terms of the number of unknowns relative to the MoM. They employ the fields generated by fictitious sources, displaced from the boundary of the scatterer, to represent the scattered field. Major concerns with these methods stem from a lack of well-defined guidelines for the selection, for arbitrarily-shaped scatterers, of the locations of the fictitious sources. Moreover, it becomes necessary in these methods to solve an oversampled system of equations by using a least squares approach, or a singular value decomposition technique [7], to obviate the numerical ill-conditioning problems of the associated matrix. A systematic examination of the ill-conditioning problem reveals that it can be traced to the isotropic nature of the elemental sources, usually employed in these approaches, because the fields radiated by these sources can be conveniently expressed in analytical forms. Recently, Pogorzelski [8] suggested the use of synthetic directive sources to represent the scattered field. The possibility of combining isotropic and directive sources has been examined by Erez and Leviatan [9]. While in [8] 2D directive sources are synthesized by arrays of isotropic sources, in [9] the directivity is achieved by shifting a point source into complex space [10]. However, in both [8] and [9], only one type of directive sources is used. This appears to be similar to the Canning's first attempts to achieve localization employing only one type of basis function as described in [2]. Thus, with the methods of [8] and [9] one can expect to achieve localization but, probably, at the expense of solving an ill-conditioned system of equations.

A new technique, called the Complex Multipole Beam Approach (CMBA), which attempts to combine the advantages of both the IML and the MMP methods has been recently introduced by the authors [11]-[12]. The strategy followed in this method is to expand the scattered fields in terms of beams, generated by a judiciously selected set of multipole sources located in the complex space. These beams are very similar to the Gabor basis functions when sampled at the boundary of the scatterer; hence, the method can be viewed as a numerical approach to finding an approximate Gabor representation of the boundary field. In

fact, the problem of radiation from planar apertures has been extensively studied using the Gabor expansion of the aperture fields [13]. However, a straightforward Gabor expansion of the field over a non-planar boundary would be of little use since the subsequent determination of the scattered field would be as difficult as solving the original problem itself. The completeness properties and other characteristics of the Gabor expansion functions are well-understood [14], and this greatly facilitates the task of developing a set of simple rules for choosing the orders and locations of the multipoles. In common with the MMP and the Current Model methods, the present approach retains its advantage over the MoM in terms of the number of unknowns, typical figures being less than four per wavelength.

The unidirectional character of the fields radiated by the multipole sources, located in the complex space, is superior to the bi-directional nature of the Gabor type of basis functions for the induced current used in the original IML approach [2], and is similar to the combined source IML approach [15]. This is because the unidirectional nature of the source fields ensures that the coupling will be low between a given source and all distant parts of the convex scatterer, including the part of the surface located on the opposite side. It also helps to suppress the spurious, interior resonance type of solutions, since the fields generated inside the scatterer are relatively low. In fact, numerical experiments have shown that the condition number of the matrix generated by using the present approach is almost independent of the shape and size of the scatterer.

In its original form [11]-[12], the CMBA approach was designed for application to the problem of scattering from large smooth bodies, with substantial savings of computer memory and time over the conventional MoM. The objective of this paper is to present a hybrid approach that extends the scope of application of the CMBA method to a more general class of scatterers. In the new approach, the problem of scattering from a complex object is first decomposed into a number of coupled problems. Each of these problems belongs to one of the following three geometrical types, each of which requires a different type of treatment: (i) large smooth boundaries between homogeneous media or perfectly electric conductors that are modeled using the CMBA method; (ii) non-smooth portions of boundaries or wires, that require a relatively small number of unknowns when modeled by using the conventional MoM; and, (iii) general inhomogeneous or otherwise complex regions that require volumetric discretization, and, hence, a relatively large number of unknowns per unit volume. The above division is equivalent to partitioning the generalized impedance matrix into blocks. Because the problems belonging to the third category require a large number of unknowns, it is desirable to reduce the number of degrees of freedom representing the coupling between each such region and the rest of the geometry. As a first step towards achieving this goal, each of the subregions belonging to the third category is enclosed in a smooth surface. Next, for sources and observation points residing outside the surface, the scattering properties

of the region are described in terms of a Beam-matrix, which is constructed numerically to relate the amplitudes of the outgoing beams to the incident field, with the beams themselves generated by multipoles located in the complex space. This formulation is analogous to the T-matrix description of scattering [16], although, thanks to the local nature of the multipole beams, the circumscribing surface is not restricted to be circular as it is in the T-matrix approach. A portion of the smooth boundary of the type-I region, included in the surface circumscribing a region of type-III, is termed a transition region. The concept of the transition region is analogous to the notion of nearest neighbor employed in the Fast Multipole Method (FMM) originated by Rokhlin [17], because the field in this region is computed directly from the equivalent currents of the type-III region. While the FMM is formulated as an iterative procedure [17]-[18], the proposed hybrid CMBA can be cast into a non-iterative form. In the direct scheme, first the interactions between all of the type-III regions are taken into account using an algorithm similar to the recursive T-matrix approach [19]. The remainder of the problem is then solved using the proposed beam formalism that takes into account the interactions between the type-III regions and the type-I smooth boundaries except for the narrow transition regions. This proposed hybrid technique, that combines the Complex Multipole-Beam approach with other conventional methods, is a versatile tool, and is expected to enhance the scope of application of the CMBA to a much wider class of problems.

The paper surveys the basic Complex Multipole-Beam approach and then describes the hybrid formulation. The application of the proposed hybrid method will be illustrated for the two-dimensional (2D), Transverse Magnetic (TM) scattering case. The dual case of transverse electric (TE) polarization, as well as the extension to three-dimensions (3D), will be dealt with in forthcoming publications.

The organization of the paper is as follows. Section 2 discusses the properties of beams generated by multipoles located in the complex space. Formulation of the method is outlined in Section 3. Details of the numerical implementation of the method and illustrative results are presented in Section 4. Finally, a few concluding remarks that summarize the paper are given in Section 5.

2. Multipole Beams and Gabor Expansion

This section is devoted to the study of the electromagnetic fields produced by multipoles with the source point shifted into the complex domain. The purpose of this study is twofold: (i) to develop an understanding of the major characteristics of the multipole fields; and, (ii) to find the parameters that adjust these characteristics in a manner such that they are optimally suited for the scattering problem at hand.

Consider a time-harmonic, two dimensional (2D) multipole source of order n located at a source point r_0 . The source can be interpreted as a singular distribution of the z -directed

uniform electric current. Let $\Psi_n(\mathbf{r}, \mathbf{r}_o)$ denote the z -directed electric field of such a source at the observation point \mathbf{r} . For a source located at the origin of the coordinate system ($\mathbf{r}_o = 0$), the field expressed in terms of polar coordinates (ρ, φ) is given by [20]

$$\Psi_n(\mathbf{r}, 0) = H_{|n|}^{(2)}(k\rho) e^{jn\varphi} \quad (1)$$

to within a constant factor suppressed herein. In (1), $H_n^{(2)}(k\rho)$ denotes the Hankel function of the second kind and order n , k is the intrinsic wavenumber, and the $e^{j\omega t}$ time dependence is implicit. In order to analytically continue (1) to the case of an arbitrary complex source point, it is necessary to express it as a single-valued analytic function that is well-defined for an arbitrary complex source point $\mathbf{r}_o = (x_o, y_o) = \mathbf{r}'_o - j\mathbf{r}''_o$, where \mathbf{r}'_o and \mathbf{r}''_o are real vectors. To this end, the following expression

$$\rho = \sqrt{(x-x_o)^2 + (y-y_o)^2} \quad \text{Re}\{\rho\} \geq 0 \quad (2)$$

that interprets ρ for an arbitrary \mathbf{r}_o was introduced [10] in the study of the zeroth-order multipole with a complex source-point. The expression under the square root in (2) vanishes at $\mathbf{r}'_o \pm \hat{z} \times \mathbf{r}''_o$ and the requirement $\text{Re}\{\rho\} \geq 0$ defines the segment connecting the two points as a branch cut. The requirement $\text{Re}\{\rho\} \geq 0$ also ensures single valued continuation of the Hankel function. It is well-known that the radiation characteristics of the zeroth-order multipole approximate those of a gaussian beam propagating in the direction of \mathbf{r}''_o with the waist located on the brunch cut [10].

Shin and Felsen [21] have proposed a derivation of the higher-order complex multipole fields based on successive derivatives of the zeroth-order multipole along the direction transverse to \mathbf{r}''_o . However, this process leads to only a partial set of multipoles, although additional multipoles can be obtained by taking the derivatives along \mathbf{r}''_o . The fields derived in this manner will comprise of either the $\sin(n\varphi)$ or $\cos(n\varphi)$ functions, which represent standing waves in the φ -direction. In this work, we propose an alternative approach, which we believe to be a simpler way to derive the higher-order multipole fields. The procedure entails a search for analytic expressions for the higher-order fields in terms of cartesian coordinates of the source and observation points. The interpretation of φ in (1) as a polar angle in the complex source point case may not be immediately apparent. However, we observe that the exponential factor is easier to continue in its entirety when rewritten as follows:

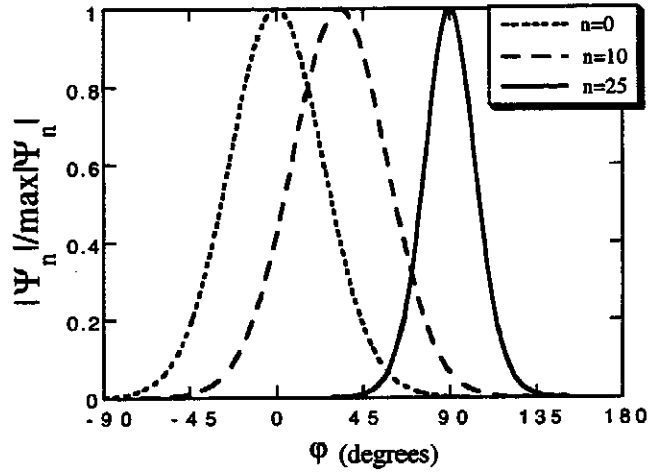
$$e^{jn\varphi} = (\cos \varphi + j \sin \varphi)^n = \left(\frac{x}{\rho} + j \frac{y}{\rho} \right)^n \quad (3)$$

Next, we define the n th order 2D multipole field as follows:

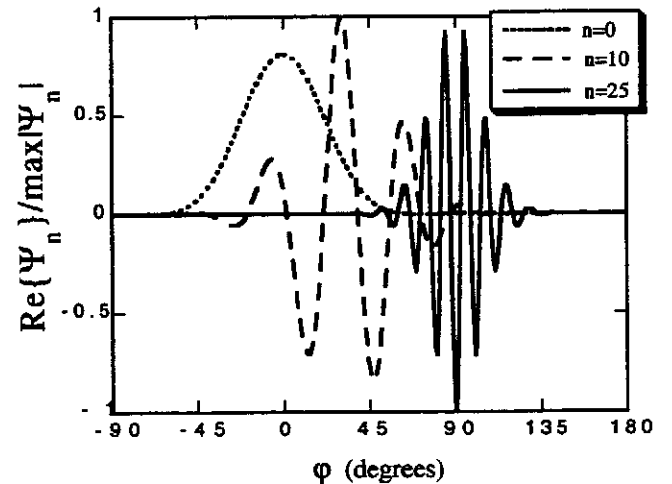
$$\Psi_n(\mathbf{r}, \mathbf{r}_o) = H_{|n|}^{(2)}(k\rho) \left(\frac{x-x_o}{\rho} + j \frac{y-y_o}{\rho} \right)^n \quad (4)$$

Equation (4), with ρ defined as in (2), is useful for constructing the n th order multipole field for arbitrary complex source coordinates.

The qualitative behavior of the multipole beams is depicted in Fig. 1 for several non-negative values of n . The negative values of n produce mirror images of their positive counterparts. Here, $|\Psi_n|$ and $\text{Re}\{\Psi_n\}$, computed on a circle of $|r| = r = 3\lambda$ in radius, λ being the wavelength, are presented as functions of φ for $\mathbf{r}''_o = 1\lambda\hat{x}$ and $\mathbf{r}'_o = 0$. Examination of the $|\Psi_n|$, shown in Fig. 1a, reveals that the complex



(a)



(b)

Fig. 1. The multipole fields $\Psi_n(\mathbf{r}, \mathbf{r}_o)$ with $\mathbf{r}_o = -j\hat{x}$ computed on a circle $|r| = r = 3\lambda$: (a) absolute value and (b) real part.

multipoles produce well-confined beams. For higher-order multipoles these beams do not propagate in the r_o'' direction. $\text{Re}\{\Psi_n\}$, shown in Figs. 1b, clearly exhibit the propagating wave behavior in the φ -direction, with an increasing spatial frequency for ascending n . The behaviors of Ψ_n on the circular contour resemble that of the Gabor expansion basis functions [3], that comprise a window function multiplied by an exponential factor. Identifying the similarity between the Gabor functions and the multipole fields is of major importance to us, as it provides us with the guidelines for selecting the parameters that play a critical role in our approach to solving the scattering problem.

The Gabor expansion of the continuous function $f(s)$ is given by

$$f(s) = \sum_{i=-\infty}^{\infty} \sum_{\ell=-\infty}^{\infty} a_{i,\ell} h_{i,\ell}(s) \quad (5)$$

where

$$h_{i,\ell}(s) = w(s - i\Delta) e^{j\ell\Omega s} \quad (6)$$

It comprises a window function $w(s)$ with an effective width W , a shift parameter Δ controlling a discrete linear shift along the s axis, and a Fourier kernel $e^{j\ell\Omega s}$ whose frequency is sampled at a constant interval Ω . For the multipole fields, the shift of the origin into the complex domain has an effect similar to that of the window function. Unlike in the Gabor expansion (5)-(6), we do not have the freedom to select the window function; however, we can adjust the free parameters W , Ω , and Δ that profoundly affect the characteristics of the complex multipole expansion. Necessary conditions for the completeness of the set of Gabor functions have been well-established and have been thoroughly studied. The conventional constraints $\Omega\Delta = 2\pi$ and $W = \Delta$, advocated by Gabor [3], are not only logical but theoretically optimal as well. However in the process of generating the approximate Gabor expansion, we have found it necessary to use a certain degree of oversampling [14], achieved by letting $\Omega\Delta < 2\pi$. As will be seen in the next section which deals with the distribution of multipole beams, we also relax the second condition and allow W to be in the range $W \geq \Delta$. In the remainder of this section, we will describe how to select a set of multipoles that approximate the set of Gabor functions $h_{0,\ell}$ centered at $s=0$. First, we choose to use only the multipoles of orders n_ℓ , $n_\ell = \ell K$, where the integer K is determined by the condition $K < 2\pi r/W$. This condition, based on an assumption that the oscillatory behavior of $e^{jn\varphi}$ is preserved, satisfies the oversampling criterion $\Omega < 2\pi/\Delta$, provided that $W \geq \Delta$. The multipole series can be truncated by limiting ℓ to the range $-L \leq \ell \leq L$, where L is the smallest integer satisfying $K(L-1) > kr$. The above condition implies that the spatial spectrum of at least one of the multipoles falls outside of the visible range.

It is evident from Fig. 1 that the multipole beams of

different orders have different widths. Following [14] we define

$$W_\ell = \frac{\int |\Psi_{n_\ell}| ds}{\max_{r \in C} |\Psi_{n_\ell}|} \quad (7)$$

as an effective width of the beam of order n_ℓ . Here, the source point is centered at the origin $r_o'' = 0$ and shifted into complex space by $r_o'' = (a_\ell \cos \alpha_\ell, a_\ell \sin \alpha_\ell)$. The contour C , along which Ψ_n is evaluated, is a smooth curve that approximates the surface of the scatterer in some average manner. Next, the amount of shift a_{q_ℓ} into the complex domain is found for each non-negative multipole of order n_ℓ such that the beams are approximately equal in their effective width, i.e. $W_\ell = W$. The direction of the complex shift of each multipole α_ℓ is chosen to ensure that the beam propagates in the x -direction. Only non-negative values of ℓ are considered, since $\alpha_{-\ell} = -\alpha_\ell$. With the choice of these carefully tuned parameters K , L , a_ℓ , and α_ℓ , the multipole fields comprise a set of analytic solutions of the wave equation which, when evaluated on a circular contour, simulate a set of Gabor basis functions. This step of constructing the above basis functions serves as a first step toward developing the formulation of the scattering problem, to be discussed in the following section.

3. FORMULATION

Consider a problem of scattering from a complex object depicted in Fig. 2. In the proposed approach our general strategy would be to decompose the problem geometry into a number of distinct regions. Each of these regions belongs to one of the following three geometrical types: (i) large smooth boundaries between homogeneous media or perfectly electric conductors; (ii) non-smooth portions of boundaries or wires; and, (iii) general inhomogeneous or otherwise complex regions that require volumetric discretization. For each of these regions we propose using a different type of modeling. In addition, coupling between the various regions

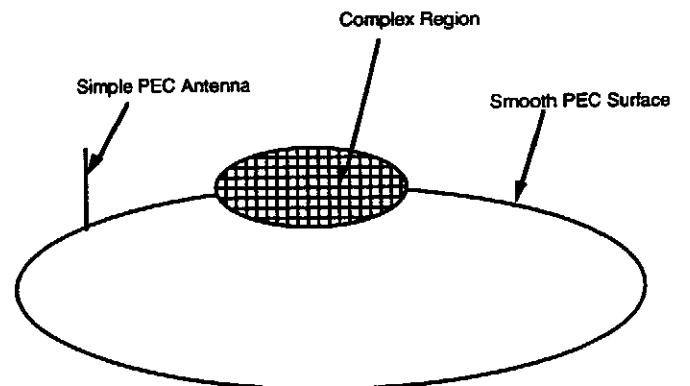


Fig. 2. An example of scattering by a general complex object.

can be formulated in a way considerably reducing the overall computational complexity of the problem in hand. The basic complex multipole beam approach (CMBA) to scattering by smooth surfaces is presented in the following subsection, while treatment of non-smooth and complex regions will be discussed, respectively in the two following subsections.

3.1 CMBA for Smooth Surfaces

For the sake of illustrating the application of the CMBA, we consider a perfectly conducting cylinder of arbitrary cross-section defined by contour S and infinite along the z -axis (see Fig. 3). The contour, which is assumed to be piecewise smooth with a minimum radius of curvature that exceeds some prescribed value r , is described by $r_c(s)$, where s is a length parameter. We also assume that $r_c(s)$ has continuous first derivatives (continuous tangent). The cylinder is illuminated by a TM (transverse-magnetic) plane wave $E^{\text{inc}} = \hat{z}E^{\text{inc}} = \hat{z}e^{-jk^{\text{inc}} \cdot r}$, where \hat{z} is a unit vector, k^{inc} denotes the wave vector of the incident field, and the harmonic $e^{j\omega t}$ time dependence is implicit. Our objective is to determine the scattered field $E^s = \hat{z}E^s$.

We begin by setting up an equivalent problem for the region surrounding the scatterer, in which we express E^s as a superposition of fields of a set of fictitious sources, located in the region originally occupied by the scatterer. Specifically, using the complex multipole sources we write

$$E^s(\mathbf{r}) = \sum_{i=1}^M \sum_{\ell=-L}^L I_{i\ell} E_{i\ell}(\mathbf{r}) \quad (8)$$

where $I_{i\ell}$ are constant coefficients to be determined and

$$E_{i\ell}(\mathbf{r}) = \Psi_{n_i}(\mathbf{r}, r_{i\ell}) \quad (9)$$

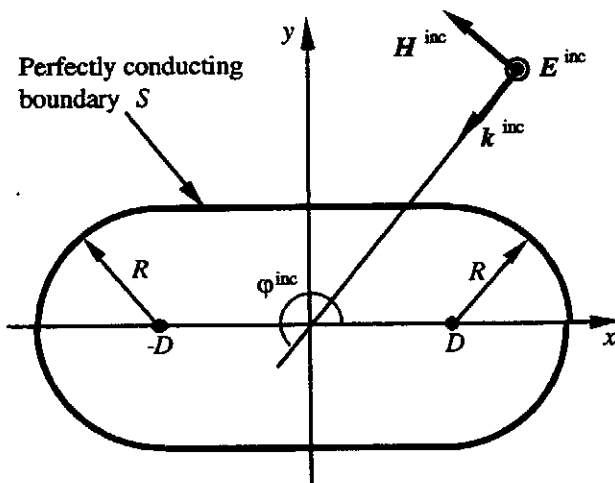


Fig. 3. An example of perfectly conducting cylinder of arbitrary smooth cross section illuminated by a TM polarized plane wave.

is the field of the multipole of order n_i , with $n_i = \ell K$, located at $r_{i\ell} = r'_i - jr''_{i\ell}$. Note that unlike in the MMP approach [5], only the multipoles whose orders are integer multiples of K are employed herein. The source locations are chosen by analogy to the Gabor expansion. The multipole centers r'_i are spaced evenly along the boundary, and are shifted an equal distance r towards the interior of the same. The value of r is selected such that it does not exceed the minimum radius of curvature. The circumference of the cylinder is divided into M segments of equal length by points s_i , $s_i = i\Delta$, $i = 1, \dots, M$. The number of multipole centers M is determined by the requirement that the length of the segments Δ be less than or equal to the predetermined effective width W of the multipole beams. The amount and direction of shift into the complex domain are determined in a manner described in the previous section. Thus, we have

$$r'_i = r_c(s_i) - \hat{n}(s_i)r \quad \text{and} \quad r''_{i\ell} = a_{|\ell|} \Re\{\alpha_\ell\} \hat{n}(s_i) \quad (10)$$

where $\hat{n}(s)$ is the unit outward normal vector at a point s on the boundary, and the operator $\Re\{\alpha\}$ denotes a rotation of $\hat{n}(s)$ by an angle α . With this distribution of sources, the boundary is fully spanned by the multipole beams. The direction of the complex shift of each of the $2L+1$ multipoles centered at r'_i ensures that the field intensity is maximum at the boundary point $r_c(s_i)$ closest to their origin. We anticipate that the similarity between the set of complex multipole beams, selected according to the procedure described in the previous section, and the Gabor basis functions is preserved for an arbitrarily smooth contour. In view of this, the representation of the scattered field given in (8) may be viewed as an approximate Gabor expansion evaluated on the scatterer boundary.

It is evident from (8), that the approximate scattered field E^s automatically satisfies both the wave equation and the radiation condition. Thus, it is only necessary to enforce the boundary condition at $N=M(2L+1)$ equispaced points on the boundary of the scatterer to derive a matrix equation which can be subsequently solved for the N unknown coefficients $\{I_{i\ell}\}$. Once these are known, the scattered fields and other quantities of interest can be readily obtained.

At this point, it would be useful to make a few observations regarding the method just outlined. First, we note that, thanks to the properties of multipole fields, the generalized impedance matrix involved is anticipated to have a very well defined structure. The matrix can be expected to be essentially banded with enhanced block-diagonal elements. This pattern is attributable to the strong coupling (reaction) between each group of $2L+1$ multipoles having a common origin and the $2L+1$ matching points closest to them. For convex scatterers, the coupling rapidly diminishes with increasing distance between the multipole origin and the match point. The banded structure of the matrix offers a number of advantages in terms of computation time and storage requirements. Additionally, we can estimate the

lower bound on the number of unknowns per linear wavelength of the contour of the scatterer. Noting that there are $2L+1$ match points per segment of length Δ , and using the constraints on the multipole parameters specified in the previous section, we can show that this bound is given by $(2L+1)/(L-1)$, which approaches the Nyquist limit of 2 unknowns per wavelength for larger L . However, large values of L can only be employed for very smooth scatterers, and even then they tend to spoil the banded structure of the matrix.

3.2 Direct Hybridization of the CMBA with the MoM

In this subsection we consider a simple way to extend the applicability of the CMBA to structures with discontinuities of the surface tangent or with simple appendages, such as wires. As an example of such geometry we consider a cylinder of a square cross-section. Here, complex multipole beams can still adequately represent the fields in the vicinity of the smooth portions of the cylinder boundary. However, they clearly can not be employed to approximate fields in the immediate vicinity of the edges. In such instances we can use conventional MoM basis functions as additional sources of the scattered field. In the case of the square cylinder the scattered field would be given by a superposition of the multipole beams and fields due to piecewise constant distributions of electric current located in the vicinity of the edges (see Fig. 4). By simple point matching, the problem can now be reduced to a matrix equation, which can subsequently be solved for the amplitudes of the multipole beams and the pulse basis functions. As the electrical size of the cylinder increases, the number of multipole beams required to span the boundary increases linearly, while the

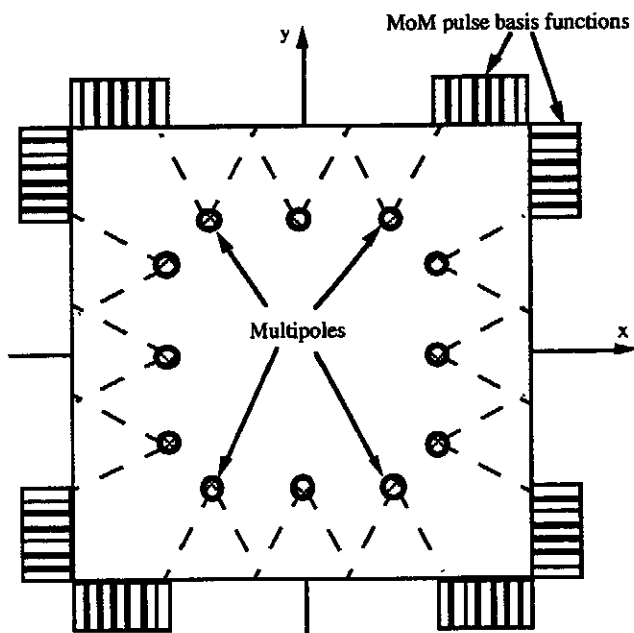


Fig. 4. An example of perfectly conducting cylinder with a square cross section illuminated by a TM polarized plane wave.

number of MoM basis functions remains unchanged. Thus, for sufficiently large problems the number of MoM basis functions, required in the edge vicinity regions, will become a small fraction of the total number of unknowns. Consequently, special treatment, like the one described in the following subsection is not justified for such regions that require a relatively small number of unknowns when modeled using the conventional MoM.

3.3 Beam-Matrix Representation of Scattering by Complex Geometries

In this subsection we consider scattering by an object comprising a large smooth boundary and a complex region that requires volumetric discretization (see Fig. 5). Such problems present special difficulties due to large numbers of unknowns involved in modeling both regions. As a first step, the complex region is enclosed in a smooth surface Ω . The main part of the large smooth boundary lying outside Ω is modeled using the CMBA. The complex region is next discretized using a volumetric MoM formulation [22]. In addition, the narrow strip of the smooth boundary within Ω is modeled using the conventional MoM. The above division mathematically corresponds to a partitioning of the generalized impedance matrix into blocks, as

$$\begin{bmatrix} Z^{ss} & Z^{st} & Z^{sc} \\ Z^{ts} & Z^{tt} & Z^{tc} \\ Z^{cs} & Z^{ct} & Z^{cc} \end{bmatrix} \begin{bmatrix} I^s \\ I^t \\ I^c \end{bmatrix} = \begin{bmatrix} V^s \\ V^t \\ V^c \end{bmatrix} \quad (11)$$

Here, superscripts "s", "t", and "c" designated quantities pertinent to smooth boundaries, transition region, and the complex region, respectively.

Accurate modeling of the inhomogeneous complex region requires a relatively large number of unknowns per unit

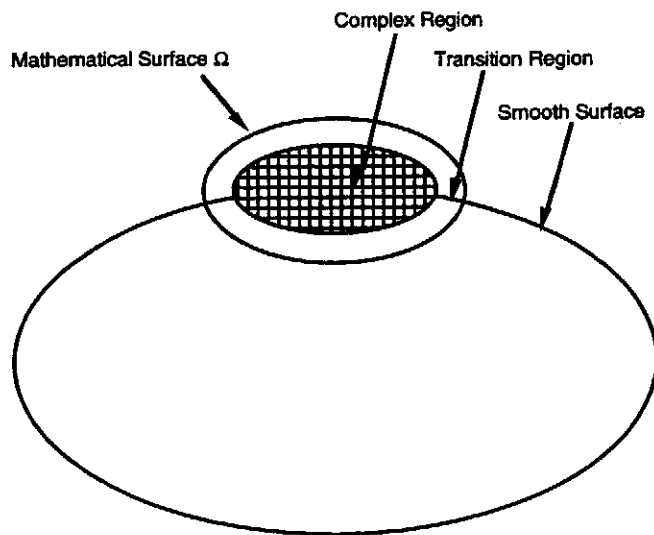


Fig. 5. An example of a scatterer comprising a smooth perfectly conducting surface and a complex region illuminated by a TM polarized plane wave.

volume. On the other hand, for observation points residing outside Ω , the scattered field due to the complex region can be represented in terms of fields of equivalent currents flowing on Ω . Similarly, the field in the complex region due to sources exterior to Ω can be simulated by another set of equivalent currents flowing on Ω . These observations motivate us in an attempt to reduce the number of degrees of freedom representing the coupling between the complex region and the rest of the geometry. Substituting $I^c = Z^{cc^{-1}}(V^c - Z^{cs}I^s - Z^{ct}I^t)$ in (11) we obtain

$$\begin{bmatrix} Z^{ss} - Z^{sc}Z^{cc^{-1}}Z^{cs} & Z^{st} - Z^{sc}Z^{cc^{-1}}Z^{ct} \\ Z^{ts} - Z^{tc}Z^{cc^{-1}}Z^{cs} & Z^{tt} - Z^{tc}Z^{cc^{-1}}Z^{ct} \end{bmatrix} \begin{bmatrix} I^s \\ I^t \end{bmatrix} = \begin{bmatrix} V^s - Z^{sc}Z^{cc^{-1}}V^c \\ V^t - Z^{tc}Z^{cc^{-1}}V^c \end{bmatrix} \quad (12)$$

where we effectively eliminated the unknowns associated with the complex region. In (12), the term $Z^{sc}Z^{cc^{-1}}Z^{cs}$ represents the coupling between the smooth boundary and the complex region. Direct computation of this term would not produce any savings. In order to facilitate its efficient evaluation we return to the above idea of equivalent representations for the fields. This time, however, we advocate the use of complex multipole beams instead of equivalent surface currents. Outside the surface Ω , the field scattered by the complex region can be represented by the fields of complex multipoles with real source points located within Ω as depicted in Fig. 6a. Similarly, the field in the complex region due to sources external to Ω can be expanded using multipole beams originating outside Ω (see Fig. 6b). With this beam representation we can write

$$Z^{sc}Z^{cc^{-1}}Z^{cs} \approx Z^{s\Omega}B^{\Omega\Omega}Z^{\Omega in^{-1}}Z^{\Omega s} \quad (13)$$

where, $Z^{s\Omega}$ is the rectangular matrix relating the field on the smooth surface to the amplitudes $I^{\Omega out}$ of the multipole beams radiating from within Ω , $Z^{\Omega s}$ is the matrix relating the incoming field $V^{\Omega in}$ on Ω to the amplitudes I^s of multipole beams associated with the smooth surface, and $Z^{\Omega in^{-1}}$ denotes the matrix transforming $V^{\Omega in}$ on Ω into the amplitudes $I^{\Omega in}$ of multipole beams radiating towards its interior. Also in (13), $B^{\Omega\Omega}$ designates the Beam-matrix of Ω defined by

$$B^{\Omega\Omega} = Z^{\Omega out^{-1}}Z^{\Omega c}Z^{cc^{-1}}Z^{c\Omega} \quad (14)$$

where, $Z^{c\Omega}$ is the rectangular matrix relating the field V^c in the complex region to the amplitudes $I^{\Omega in}$ of the multipole beams radiating into Ω , $Z^{\Omega c}$ is the matrix relating the outgoing field $V^{\Omega out}$ on Ω to the coefficients I^c of basis functions associated with the complex region, and $Z^{\Omega out^{-1}}$ denotes the matrix transforming the $V^{\Omega out}$ into the amplitudes $I^{\Omega out}$ of multipole beams radiating towards

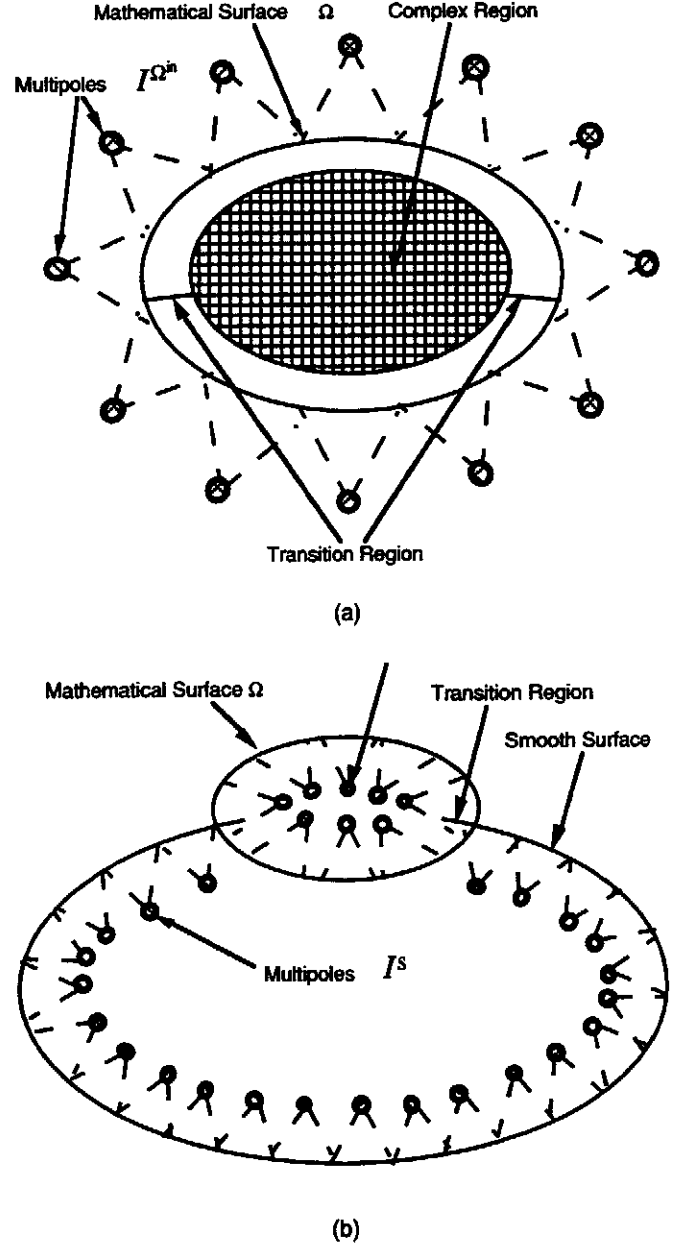


Fig. 6. Equivalent situations for (a) the interior and (b) the exterior of the surface Ω .

its exterior. The entire process of computing $Z^{sc}Z^{cc^{-1}}Z^{cs}$ is illustrated in Fig. 7. In this formulation the scattering properties of the complex region are fully described in terms of a Beam-matrix, which relates the amplitudes of the outgoing beams to the those of the incoming ones. This formulation is analogous to the T-matrix description of scattering [16], although, thanks to the local nature of the multipole beams, the circumscribing surface is not restricted to be circular as it is in the T-matrix approach. A portion of the smooth boundary, included in the surface circumscribing the complex region, is termed a transition region. The concept of the transition region is analogous to the notion of the nearest neighbor employed in the fast multipole

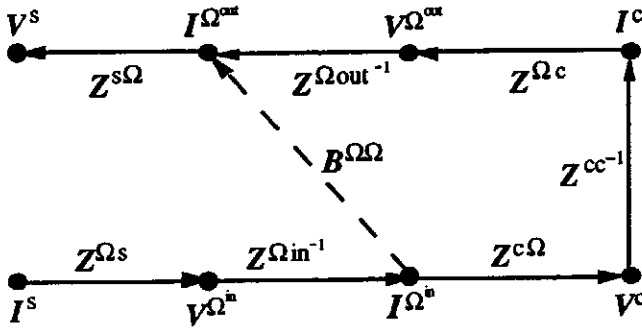


Fig. 7. Schematic diagram illustrating the computation of the coupling term between the smooth surface and the complex region.

algorithm of Rokhlin [17], because the field in this region is computed directly from the equivalent currents of the complex region. In the direct scheme presented herein, the interactions between all of the complex regions are taken into account first using an algorithm similar to the recursive T-matrix approach [19]. The remainder of the problem is then solved using the proposed beam formalism that takes into account the interactions between the complex regions and the rest of the scatterer geometry, viz., the smooth boundaries except for the narrow transition regions and simple regions modeled using the MoM as described in the previous subsection.

4. NUMERICAL RESULTS

The formulation presented in the preceding section has been implemented in a versatile computer program. In this section, we present the computed results for several scatterers with shapes that gradually increase in complexity. The accuracy of the proposed method is verified by comparing our numerical results with those obtained by using the conventional MoM. Internal validity check is additionally provided by evaluating the error in the satisfaction of the boundary condition on the surface of the scatterer at locations between the match points.

In all of the computations, presented herein, we have employed the same basic set of multipole beams. We begin by optimizing the parameters of the multipoles producing these beams. We displace the multipole centers by $r=3\lambda$ from the scatterer surface and choose a beamwidth of $W=3.5\lambda$ as a compromise between a reasonable directivity and locality of the interaction. For the contour C we choose a circle 6λ in radius for the effective width computation as in (7). The center of C is offset in the negative x -direction by 3λ away from the multipole origin. For these choices, we then optimize the remaining parameters by following the procedure described towards the end of Section 2. To ensure sufficient oversampling, we choose $K=5$ and, consequently, $L=5$.

The results obtained by following the above procedure are presented in Table I. The width of the highest order multipole, with $n_5=25$, was 3.42λ and it could not be

Table I. Multipole parameters optimized for $W=3.5\lambda$, $r=3\lambda$, and $K=5$.

ℓ	n_ℓ	a_ℓ/λ	α_ℓ (degrees)	W_ℓ/λ
0	0	0.91	0	3.49
1	5	0.92	16	3.49
2	10	0.95	33	3.50
3	15	1.17	57	3.50
4	20	0.58	85	3.50
5	25	0.001	90	3.42

made equal to 3.5λ even by letting $a_5 \rightarrow 0$. This was because, in this case, the effective width is bounded by the evanescent behavior of the field and not by its directivity achieved by the complex shift of the origin.

The first problem considered is that of a perfectly conducting cylinder as depicted in Fig. 3 with $R=6\lambda$ and $2D=\pi R$. This problem allows us to exemplify the main features of the CMBA when applied to scattering from smooth perfectly conducting objects, as discussed in Subsection 3.1. For this case we used 22 multipole origins each with the same 11 multipoles, with a total of $N=242$ unknowns, which average out to 3.2 unknowns per wavelength, which is only slightly higher than the lower bound derived in the previous section ($(2L+1)/(L-1)=2.75$ for $L=5$). The structure of the resulting matrix is depicted in Fig. 8. Each column of the matrix is normalized to unity maximum element. The convex shape of the scatterer results in a low coupling between distant sources and matching points, and this is evident from the sparse and approximately banded structure of the matrix. We have found that the elements with the absolute value smaller than 10^{-3} can be set to zero without any significant loss of accuracy. The bandwidth of non-zero elements in the matrix becomes approximately 120 when this is done. In view of this, we estimate that for a convex scatterer the storage requirement will only be on the order of $120N$, and, consequently, will result in a reduction of computation time. The condition number for this example was 321, a very low value that compared very favorably with those obtained in the conventional CM method and the MMP. The rms boundary condition error was only about 0.5%. A comparison was also made between the scattering cross section results computed by our method and those obtained by using the MoM with 800 unknowns. These results are shown in Fig. 9 for the case of $\phi^{inc}=90^\circ$. Complete agreement between the two also serves as an evidence of the accuracy of the CMBA.

Next, we consider scattering from a perfectly conducting square cylinder with a side length of 12λ . This case will illustrate the hybridization of the CMBA with the MoM for objects with not entirely smooth boundaries, as discussed in Subsection 3.2. The total number of $N=132$ multipoles were distributed between $M=12$ origins so as to span the

